

Geophysical Research Letters[®]



RESEARCH LETTER

10.1029/2022GL102341

Key Points:

- This eruption produced the most intense lightning rates ever documented in Earth's atmosphere
- Lightning rings expand with enormous gravity waves in the umbrella cloud, caused by buoyant oscillation of the overshooting plume top
- Volcanic lightning and satellite analysis reveal at least four phases of eruptive activity from 02:57–15:12 UTC on 15 January 2022

Supporting Information:

Supporting Information may be found in the online version of this article.

Correspondence to:

A. R. Van Eaton,
avaneaton@usgs.gov

Citation:








Van Eaton, A. R., Lapierre, J., Behnke, S. A., Vagasky, C., Schultz, C. J., Pavlonis, M., et al. (2023). Lightning rings and gravity waves: Insights into the giant eruption plume from Tonga's Hunga Volcano on 15 January 2022. *Geophysical Research Letters*, 50, e2022GL102341. <https://doi.org/10.1029/2022GL102341>

Received 6 DEC 2022
Accepted 21 APR 2023

Author Contributions:

Conceptualization: Alexa R. Van Eaton, Jeff Lapierre, Sonja A. Behnke, Chris Vagasky, Christopher J. Schultz
Data curation: Alexa R. Van Eaton, Jeff Lapierre, Sonja A. Behnke, Chris Vagasky, Christopher J. Schultz, Kristopher Bedka, Konstantin Khlopenkov

Lightning Rings and Gravity Waves: Insights Into the Giant Eruption Plume From Tonga's Hunga Volcano on 15 January 2022

Alexa R. Van Eaton¹ , Jeff Lapierre², Sonja A. Behnke³ , Chris Vagasky^{4,5} , Christopher J. Schultz⁶ , Michael Pavlonis⁷ , Kristopher Bedka⁸ , and Konstantin Khlopenkov⁹ 

¹U.S. Geological Survey, Cascades Volcano Observatory, Vancouver, WA, USA, ²Advanced Environmental Monitoring (AEM), Germantown, MD, USA, ³Electromagnetic Sciences and Cognitive Space Applications, Los Alamos National Laboratory, Los Alamos, NM, USA, ⁴Vaisala Inc., Louisville, CO, USA, ⁵Now at Department of Agronomy, University of Wisconsin, Madison, WI, USA, ⁶NASA Marshall Space Flight Center, Huntsville, AL, USA, ⁷National Oceanic and Atmospheric Administration (NOAA)/National Environmental Satellite, Data, and Information Service (NESDIS) Center for Satellite Applications and Research, Advanced Satellite Products Branch, Madison, WI, USA, ⁸NASA Langley Research Center, Hampton, VA, USA, ⁹Science Systems and Applications, Inc, Hampton, VA, USA

Abstract On 15 January 2022, Hunga Volcano in Tonga produced the most violent eruption in the modern satellite era, sending a water-rich plume at least 58 km high. Using a combination of satellite- and ground-based sensors, we investigate the astonishing rate of volcanic lightning ($>2,600$ flashes min^{-1}) and what it reveals about the dynamics of the submarine eruption. In map view, lightning locations form radially expanding rings. We show that the initial lightning ring is co-located with an internal gravity wave traveling >80 m s^{-1} in the stratospheric umbrella cloud. Buoyant oscillations of the plume's overshooting top generated the gravity waves, which enhanced turbulent particle interactions and triggered high-current electrical discharges at unusually high altitudes. Our analysis attributes the intense lightning activity to an exceptional mass eruption rate ($>5 \times 10^9$ kg s^{-1}), rapidly expanding umbrella cloud, and entrainment of abundant seawater vaporized from magma-water interaction at the submarine vent.

Plain Language Summary The eruption of Tonga's underwater Hunga Volcano culminated on 15 January 2022 with a giant volcanic plume that rose out of the ocean and into the mesosphere. This plume created record-breaking amounts of volcanic lightning observed both from space and by radio antennas on the ground thousands of kilometers away. We show that the eruption created more lightning than any storm yet documented on Earth, including supercells and tropical cyclones. The volcanic plume rose to its maximum height and expanded outward as an umbrella cloud, creating fast-moving concentric ripples known as gravity waves, analogous to a rock dropped in a pond. Point locations of lightning flashes also expanded outward in a pattern of donut-shaped rings, following the movement of these ripples. Optically bright lightning was detected at unusually high altitudes, in regions of the volcanic cloud 20–30 km above sea level. Our findings show that a sufficiently powerful volcanic plume can create its own weather system, sustaining the conditions for electrical activity at heights and rates not previously observed. Overall, remote detection of lightning contributed to a detailed timeline of this historic eruption and, more broadly, provides a valuable tool for monitoring and nowcasting hazards of explosive volcanism worldwide.

1. Introduction

An explosive eruption began on 19 December 2021 (coordinated universal time, UTC) near the remote islands of Hunga Tonga and Hunga Ha'apai in the South Pacific Ocean (Carr et al., 2022; Gupta et al., 2022). These two islands are small peaks on the rim of a much larger submarine caldera volcano known as Hunga Volcano (Taaniela Kula, Tonga Geological Services, written communication, 10 September 2022). The explosive activity intensified on 13 January 2022 (UTC), followed by the climactic eruption on 15 January that sent a water-rich volcanic plume into the mesosphere (Carr et al., 2022; Podglajen et al., 2022; Proud et al., 2022). This event continues to push the boundaries of our understanding of how explosive volcanism impacts the broader Earth system. In addition to significant local impacts on the Kingdom of Tonga (Purkis et al., 2023), the eruption created global-scale acoustic waves (Matoza et al., 2022), tsunamis (Omira et al., 2022), ionospheric and geomagnetic disturbances

© 2023 The Authors. This article has been contributed to by U.S. Government employees and their work is in the public domain in the USA.

This is an open access article under the terms of the [Creative Commons Attribution License](https://creativecommons.org/licenses/by/4.0/), which permits use, distribution and reproduction in any medium, provided the original work is properly cited.

Formal analysis: Alexa R. Van Eaton, Jeff Lapierre, Sonja A. Behnke, Chris Vagasky, Christopher J. Schultz, Michael Pavolonis, Kristopher Bedka, Konstantin Khlopenkov

Methodology: Alexa R. Van Eaton, Jeff Lapierre, Sonja A. Behnke, Chris Vagasky, Christopher J. Schultz, Michael Pavolonis, Kristopher Bedka, Konstantin Khlopenkov

Visualization: Alexa R. Van Eaton, Jeff Lapierre, Sonja A. Behnke, Kristopher Bedka, Konstantin Khlopenkov

Writing – original draft: Alexa R. Van Eaton

Writing – review & editing: Alexa R. Van Eaton, Jeff Lapierre, Sonja A. Behnke, Chris Vagasky, Christopher J. Schultz, Michael Pavolonis, Kristopher Bedka, Konstantin Khlopenkov

(Astafyeva et al., 2022; Gavrilov et al., 2022), and warmed the climate due to water vapor injection (Sellitto et al., 2022). Additionally, Briggs et al. (2022) noted the high rates of volcanic lightning during this eruption, leading to key questions about the nature of electrification during such an extreme event. Here, we examine the evolution of the volcanic plume and its extraordinary lightning activity. Although we focus primarily on 15 January, we also provide a data set of lightning characteristics from 13 to 14 January for future research.

2. Data and Methodology

2.1. Volcanic Plume Observations

The volcanic plume on 15 January 2022 was characterized using visible and infrared observations from two geostationary satellites: GOES-17 (operated by the U.S. National Oceanic and Atmospheric Administration, NOAA) and Himawari-8 (Japan Meteorological Agency). All times are reported in UTC (local Tonga Time is UTC +13 hr). Our analysis accounts for the ~7 min difference between the scan start and the timing of the scan line over Hunga Volcano for both satellites. This time offset means that the 04:00 image does not record observations near the volcano until 04:07, which has important implications for establishing the chronology of the eruption.

We retrieved stereoscopic cloud heights from the combination of nearly synchronous satellite images at 10-min intervals using 10.3- μ m band infrared brightness temperatures from GOES-17 and Himawari-8, as described in Podglajen et al. (2022). These height retrievals are accurate within ± 0.5 km and eliminate the effects of parallax related to the viewing angle of individual satellites. However, the analysis was limited to clouds >10 km above sea level (asl) and within a $\sim 1,920 \times 1,080$ km grid around the volcano. Maximum plume heights were extracted within 100 km of Hunga Volcano for the first 7 hours of eruption and within 50 km thereafter. The lower-level plumes occurring early on 15 January were estimated using shadow lengths or minimum brightness temperatures matched to atmospheric temperatures (Oppenheimer, 1998) with uncertainties of ± 3 km (Figure S2 in Supporting Information S1). Volcanic cloud areas were determined from the stereopairs from 04:17–07:07 and NOAA's GOES-17 based volcanic cloud detection and tracking product (Pavolonis et al., 2018) from 07:17–16:07 (Van Eaton et al., 2023). We use the term *umbrella cloud* to refer to a density-driven, horizontal intrusion into the atmosphere (Sparks et al., 1997: Ch. 11).

2.2. Lightning Detection and Analysis

Several long-range systems detected the lightning from this eruption (Text S1, Table S1 in Supporting Information S1). First, we obtained data from the satellite-based Geostationary Lightning Mapper (GLM) onboard GOES-17. GLM uses pixel mapping to obtain the timing, location, flash area, and optical brightness of lightning. Next, we created a combined data set from three ground-based networks of radio antennas: (a) Vaisala's Global Lightning Data set (GLD360), and (b) the Earth Networks Total Lightning Network (ENTLN), which incorporates data from (c) the World Wide Lightning Location Network (WWLLN). These systems detect radio waves emitted by impulsive discharges of electrical current, known as *pulses*, which occur intermittently throughout a lightning flash. Data include the timing, latitude, longitude, and estimated peak current of each lightning pulse. A lightning *flash* may consist of multiple pulses, which can be grouped together using temporal and spatial constraints (e.g., Cummins et al., 1998). For this study, pulses from the ground-based networks were combined into a single data set. Duplicates were removed if they occurred within 100 μ s and 5 km of a prior pulse. Then the pulses were clustered into lightning flashes serially by requiring the time between successive pulses to be no more than 100 ms and the total flash duration to be no more than 1 s. To be included in the flash, a pulse was required to be ≤ 10 km from at least one other pulse in the flash (see Text S2 and Figure S2 in Supporting Information S1).

To minimize lightning contamination from non-volcanic storms, we identified nearby convective cells that did not originate from Hunga Volcano using GOES-17 multispectral imagery through NASA's Worldview platform. This process was relatively straightforward for 15 January, leading to the following constraints on volcanic lightning: (a) within 250 km of the volcano for optical GLM observations, (b) within 300 km for ground-based observations, and (c) constrained to 00:00–15:12 for all data. Although this paper focuses on the 15 January activity, we also include lightning data from 13 to 14 January 2022 to provide a complete data set for future researchers. We caution that there was substantially more complex storm activity on 13–14 January that merged with the volcanic clouds. We have not attempted to quantify or remove the non-volcanic lightning on those days, which will require careful attention in future work.

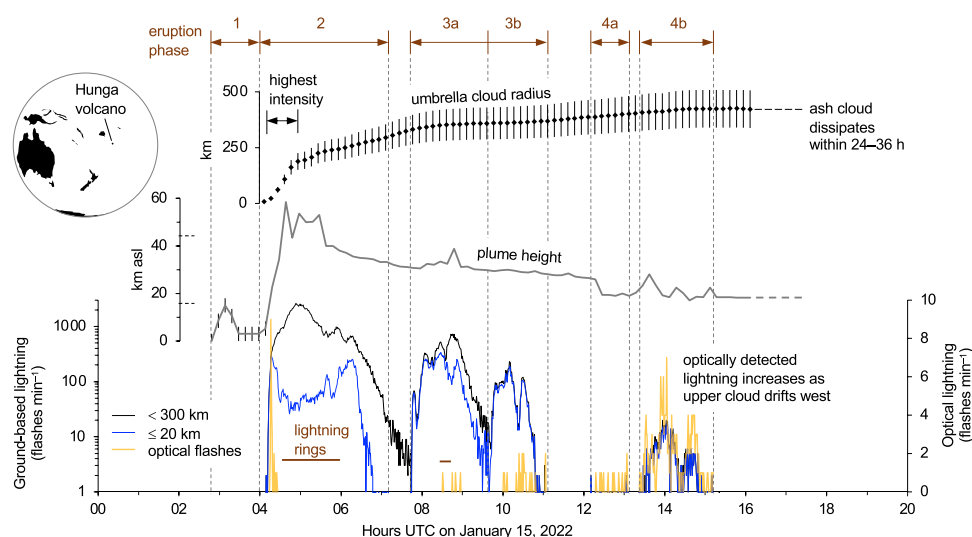


Figure 1. Satellite and volcanic lightning chronology of the 15 January 2022 eruption of Hunga Volcano in Tonga. Four phases of eruptive activity can be distinguished using umbrella cloud growth, maximum plume heights, and lightning rates. Lightning detected by ground-based networks is shown on the left axis (log scale) in terms of flashes min^{-1} occurring within 300 km (black line) and 20 km of the volcano (blue line). Optically detected flash rates (yellow bars) are shown on the right axis (linear scale) and include lightning detected within 250 km of the volcano. Timing of lightning rings indicated by two horizontal lines. Details of each eruption phase on 15 January are provided in Table S2 in Supporting Information S1. Heights of the tropopause (~ 17 km) and stratopause (~ 43 km) are shown as dashed lines on the plume height axis, given in km above sea level (asl). See Figure S3 in Supporting Information S1 for meteorological sounding data.

Key issues related to the configuration of each detection system are described in the Text S1, Figure S1, and Table S1 in Supporting Information S1. One limitation is that unusually high flash rates saturated the GLD360 sensors from 04:30 to 06:00 on 15 January. During this time the system prioritized detection of higher-current lightning, which meant that many of the low-current pulses were lost. These effects show up clearly in the lightning locations within 20 km of the volcano as an apparent dip in proximal flash rates (Figure 1, Figure S1 in Supporting Information S1).

3. Results and Analysis

3.1. Chronology of Eruptive Activity on 15 January

The timelines of plume heights, umbrella cloud growth, and lightning flash rates reveal distinct phases of eruptive activity on 15 January (Figure 1, Table S2 in Supporting Information S1). Significant airborne emissions lasted for at least 11 hr. Phase 1 began with an initial volcanic plume visible in satellite images by 02:57. The plume rose briefly to ~ 15 km (based on shadow lengths) before returning to lower altitudes by 03:20 and persisting through 03:57. There was no lightning detected yet. A sudden increase in the plume's width occurred in the 04:07 satellite images. Vergoz et al. (2022) identified the onset of long-range infrasound at 04:00, and we suggest that a step-change in the eruption dynamics may have led to a larger, higher velocity plume at this time. Phase 2 encompasses the most intense stage of the eruption from 04:00–07:11, with mass eruption rates (flux of magma, magmatic gas, and vaporized seawater) exceeding $5 \times 10^9 \text{ kg s}^{-1}$ from 04:15–04:57 based on the rate of umbrella growth (Text S3, Figure S4 in Supporting Information S1). The plume rose to a maximum overshoot of 58 km and expanded into at least two atmospheric levels, as noted by Carr et al. (2022) and Gupta et al. (2022). The upper umbrella intruded into the stratosphere (reaching 30–40 km and higher) while a second, lower cloud spread out at the level of the tropopause (but with cloud tops reaching ~ 20 km). A renewed phase of eruptive activity began at 07:46 with the return of proximal lightning and an overshooting top 39 km high by 08:47 (Figure 1). Phase 4 represents lower-level activity with an overshoot of 28 km at 13:37. Based on the end of proximal volcanic lightning, we estimate the eruption ended around 15:12.

3.2. Comparison of Lightning From Radio and Optical Systems

One striking observation is the gap in optically detected lightning just as plume heights and lightning rates from ground-based radio frequency systems reached their peak (Figure 1, Figure S5 in Supporting Information S1).

The earliest lightning on 15 January was detected by ground-based systems at ~04:09 as the plume ascended rapidly from 5 to 23 km asl. GLM observed 22 optical flashes from 04:14–04:25, which became gradually smaller and dimmer as the plume continued to rise (flash size decreased from 8,243 to 4,487 km² and optical energy decreased from 1,543 to 86 fJ). The lightning became undetectable by GLM as the plume rose above ~30 km asl despite the dramatic increase in flash rates from ground-based networks (Figure 1; eruption Phase 2). These observations suggest two different possibilities. One is that lightning may have occurred only below ~30 km and the optical energy could not penetrate the overlying cloud (Schultz et al., 2020). Alternatively, it is possible that lightning did continue throughout the entire cloud, but at heights above ~30 km the flashes were too small or optically dim to be detected by GLM (cf. Cummins, 2021; Rison et al., 2016). However, we do not favor this explanation because the very high peak currents detected from 04:30–05:40 (Figure S1 in Supporting Information S1) suggest that any traditional lightning occurring near the cloud top would have been optically bright (Quick & Krider, 2013). We explore these concepts further in Section 4.3.

By 05:37, the eruptive intensity weakened enough that stratospheric winds began to shear off the upper umbrella and reveal parts of the lower cloud below (see Figure 2 and Figure S3 in Supporting Information S1). Yet optical detections did not resume until 4 hours later (at 08:32) during a phase of renewed activity (phase 3a; Figure 1). Lightning could only be optically detected in regions of the cloud below ~30 km during this phase, determined by mapping the GLM flashes onto stereoscopic cloud height retrievals (Figure 2, Figure S5 in Supporting Information S1, Movie S1). The greatest number of optically detected flashes occurred from 12:17–15:21 once the upper umbrella drifted away from Hunga Volcano and exposed the core of the volcanic plume directly above the vent. The size of GLM flashes also reached their peak during this time (~20,000 km²) even though cloud tops were much lower than earlier in the eruption (17–28 km asl; Figure 2).

3.3. Gravity Waves and Lightning Rings in the Expanding Umbrella Cloud

It is common for strong thunderstorms, wildfire plumes, and volcanic plumes to produce an overshooting top that oscillates around the level of neutral buoyancy, sending out concentric gravity waves like ripples from a rock dropped into a pond (e.g., Apke et al., 2018; Bonadonna & Phillips, 2003; Holasek et al., 1996; Luderer et al., 2007). The Hunga eruption took this process to the extreme. Its overshooting dome was more than 100 km across and rose to 58 km asl by 04:37, then dropped to 30 km asl over the next 10 min (Figure 1, Figure S4 in Supporting Information S1). By 04:47, the resulting gravity wave was >10 km high from peak to trough and moved outward at speeds >80 m s⁻¹ (Figure S6 in Supporting Information S1). The vertical motion of this gravity wave superimposed on the lateral expansion of the density-driven umbrella cloud, which moved outward at rates of 60–90 m s⁻¹ from 04:27 to 04:47. For context, winds this strong at ground level (>130 miles hr⁻¹) would uproot large trees and cause catastrophic damage. In map view, the ground-based lightning locations reveal successive, radially expanding rings of electrical activity. The overlay of stereoscopic cloud heights and lightning locations show that the first and largest ring is co-located with the leading edge of the first and largest gravity wave in the upper umbrella cloud (see 04:16–04:52 in Figure 2, Movie S1).

4. Discussion

4.1. What Caused the Lightning Rings?

The initial lightning ring concentrated at the leading edge of an enormous gravity wave in the stratospheric umbrella cloud (Figure 2, Movie S1). This feature-matching suggests the lightning ring occurred predominantly in the upper umbrella rather than in the lower-level portion of the cloud that spread out near the tropopause. Lightning rings (also known as lightning holes) have been observed in severe storms before (Calhoun et al., 2013, 2014; Payne et al., 2010), but never associated with convective gravity waves, nor on this scale (~140 km radius for Hunga's largest ring compared to ~10 km in severe storms). It is possible that a distinct mechanism governed ring formation in this case.

We propose that the lightning radiated outward in a concentric pattern because it was modulated by turbulence and air pressure changes induced by gravity wave propagation. Updrafts associated with the transverse (i.e., vertical) motion of the gravity waves—combined with horizontal expansion of the density-driven umbrella region—would have provided a source of particle motion to organize and separate regions of charge. Numerical simulations have shown that gravity waves from overshooting tops in wildfire plumes can induce turbulence and sharp gradients in air pressure and particle concentration (Luderer et al., 2007). Hunga's fast-moving gravity waves likely

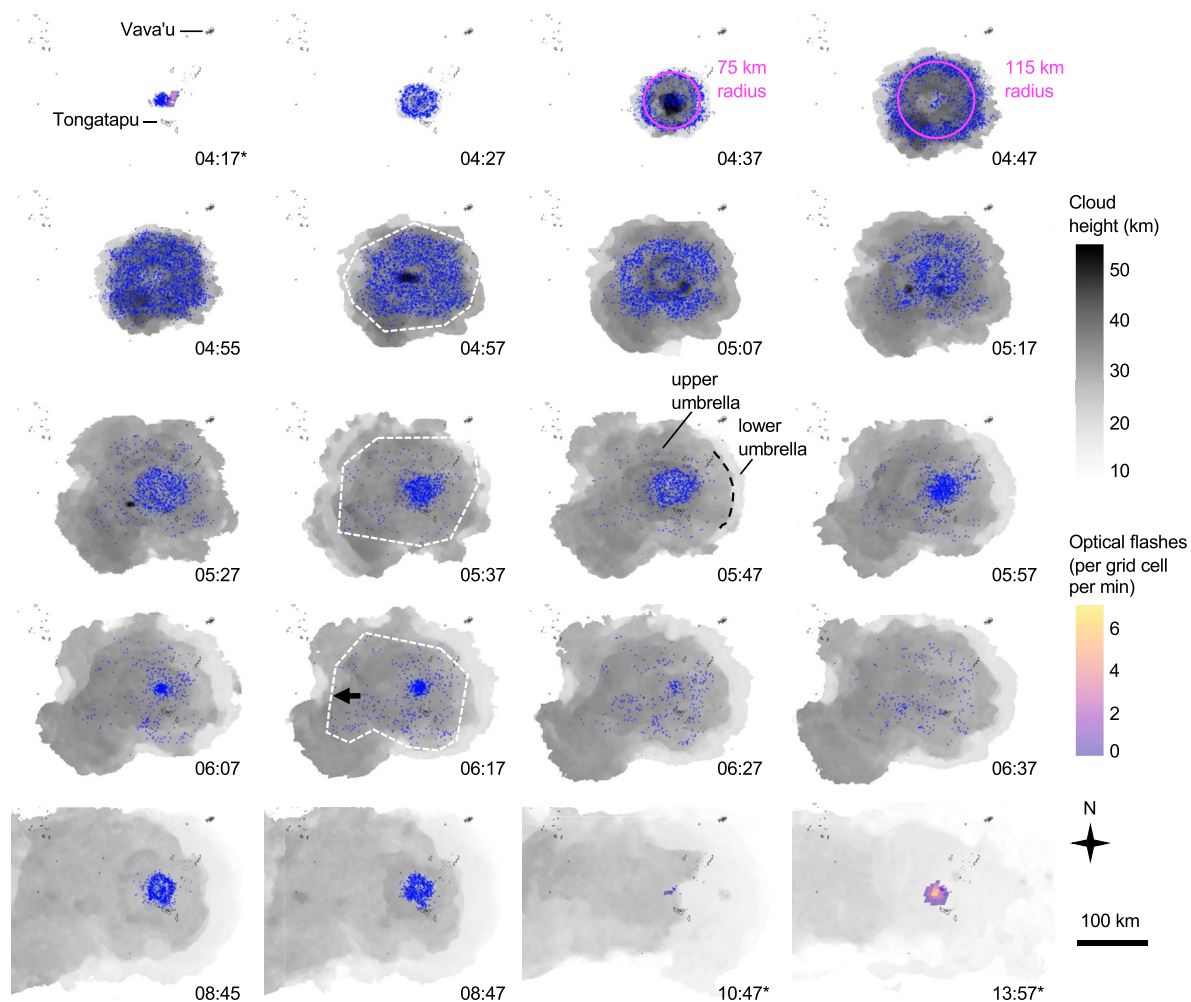


Figure 2. Maps of volcanic plume and lightning development on 15 January 2022, with times shown in UTC. Grayscale gives stereoscopic cloud heights, blue dots show lightning flashes detected by ground-based radio frequency networks over the following minute, and purple-yellow color scale shows optically detected lightning from the GLM sensor. (*) indicates frames with optically detected lightning. At least four distinct lightning rings occur from 04:16 to 05:51 followed by a final ring from 08:38–08:48. The initial and most prominent ring (visible in the first four frames) concentrated at the leading edge of a gravity wave within the upper umbrella cloud. Pink circles outline the lightning ring in two frames, showing an (average) expansion rate exceeding 60 m s^{-1} . Westward advection of the upper umbrella starts to reveal a lower level cloud by 05:37. White dashed polygons outline the lightning locations, showing their westward movement with the stratospheric umbrella cloud. Local islands are outlined in black.

segregated the particles by size (and thus, electric charge) depending on how they coupled to the flow. These processes seem to have preferentially occurred at the wave front, creating lightning in a circular pattern. As the wave moved through, it triggered enough lightning to neutralize the charge locally, explaining the lightning “hole” from 04:37 to 04:47 (Figure 2). Yet 2 minutes later, the gap begins filling in, apparently from the ring inward (Movies S1, S2)—we do not currently have a satisfactory explanation for this phenomenon. Future studies of the mechanisms behind these unique observations would benefit from a three-dimensional, non-hydrostatic model of volcanic plume electrification. However, such a model does not yet exist (cf. Textor et al., 2006).

4.2. Why Was the Lightning Activity So Intense?

Our analysis demonstrates that the 15 January eruption produced $2,615 \text{ flashes min}^{-1}$ at its peak intensity (04:53), representing the most intense electrical storm ever detected by global networks (Table S3 in Supporting Information S1). This peak lightning rate is significantly higher than the next most lightning-rich case study in our analysis (cf. $993 \text{ flashes min}^{-1}$, Table S3 in Supporting Information S1). What made this eruption so intensely electrified?

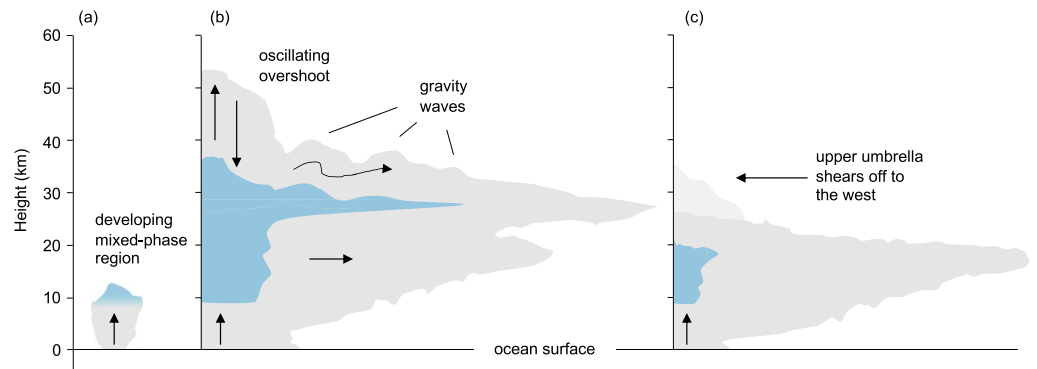


Figure 3. Conceptual sketch of dynamic and microphysical processes in the volcanic plume on 15 January 2022. Plume top morphologies are based on transects through the stereoscopic cloud height retrievals (Figure S6 in Supporting Information S1), whereas the underlying structure is inferred. Blue shading indicates the mixed phase zone, where liquid water, cloud ice, graupel, and ash coexist—this is where we expect most of the lightning to occur. (a) Represents the developing plume before lightning was detected (before 04:09 UTC); (b) represents the plume at its maximum height > 50 km when oscillation of the overshooting top sent out gravity waves through the upper umbrella (04:37–05:27); (c) represents the waning eruption as the upper umbrella detached and drifted west (after 05:37).

Previous studies have shown that volcanic plumes become electrified in two ways: (a) silicate charging from ash particle breakup and collisions and (b) ice charging, which is analogous to regular thunderstorm electrification (Mather & Harrison, 2006; Cimorelli et al., 2022, and references therein). The submarine location of Hunga's vent allowed the eruption to vaporize vast amounts of seawater, transporting an unprecedented 50–150 Tg of water vapor into the stratosphere (Millán et al., 2022; Vömel et al., 2022). In general, “wet” eruption plumes start at magmatic temperatures ($\sim 1000^{\circ}\text{C}$) and cool during explosive mixing with surrounding water (Koyaguchi & Woods, 1996). The high initial velocity and heat budget of major volcanic eruptions allow them to penetrate much higher into Earth's atmosphere compared to severe thunderstorms (Herzog & Graf, 2010; Sparks et al., 1997; Woods, 1995). Ice charging occurs when a plume creates strong updrafts through a mixed phase region containing liquid and frozen hydrometeors. These conditions are much more likely to arise in large volcanic plumes created by magma-water interaction (e.g., Behnke et al., 2013; Prata et al., 2020; Van Eaton et al., 2012, 2020, 2022) because the added water leads to high concentrations of liquid and frozen hydrometeors in the upper plume. In fact, large-eddy simulations show that it is theoretically possible to sustain liquid water in the warm interior of an eruption column well into the stratosphere (Van Eaton et al., 2012; their Figure 3). Therefore, our observations of optically detected lightning up to 20–30 km asl (Section 3.2, Figure S5 in Supporting Information S1) suggest that the lightning-producing, mixed-phase region of Hunga's plume may have also extended up to ~ 30 km high. Figure 3 shows a conceptual sketch of a mixed-phase microphysical zone in the warmer core of the plume, carrying liquid water, icy hydrometeors, and ash into the mid- to upper stratosphere.

However, it is not just the plume's water content that produced the extraordinary storm. Volcanic lightning rates scale with eruptive intensity—taller plumes and broader umbrella clouds produce more flashes (e.g., Behnke et al., 2013; Smith et al., 2021; Van Eaton et al., 2022). The Hunga eruption shows positive relationships among flash rate, plume height, and umbrella expansion through time on 15 January (Figure S4 in Supporting Information S1). In supercell thunderstorms, flash rates are correlated with both the updraft mass flux and the flux of precipitating ice (graupel) due to increased hydrometeor collisions (Deierling et al., 2008; Kulman et al., 2006). Turbulence creates a clumpy distribution of charge that supports higher flash rates due to the increase in high electric field regions at the boundaries of charge pockets (Bruning & MacGorman, 2013). Flash rates have been shown to correlate with turbulent kinetic energy (Behnke & Bruning, 2015; Bruning & MacGorman, 2013). Therefore, it is likely the high mass flux in Hunga's volcanic plume ($> 5 \times 10^9 \text{ kg s}^{-1}$ by our calculations) encouraged more turbulent inter-particle collisions that enhanced charge generation.

4.3. Evidence of Stratospheric Lightning Initiation?

Optically bright lightning was detected by the GLM sensor in regions of the volcanic plume as high as 20–30 km asl (Movies S1, S2, Figure S5 in Supporting Information S1). Although there are large uncertainties on these

estimates, the possibility of lightning at such high altitudes is intriguing. Previous studies have only detected lightning initiation processes up to ~ 18 km asl in overshooting cloud tops (DiGangi et al., 2016; MacGorman et al., 2017). In Earth's atmosphere, it becomes easier for electrical breakdown to occur at higher altitudes, but more difficult to create the hot plasma channels (leaders) that characterize lightning (Dwyer & Uman, 2014). For example, electrical phenomena known as blue jets and gigantic jets begin as lightning leaders propagating out of a thundercloud top, but only the cold plasma (streamer zone) propagates into the mid stratosphere and beyond (Krehbiel et al., 2008). The theoretical limit on this streamer-to-leader transition in Earth's atmosphere is 20–23 km asl, due in part to the very low air densities at high altitude, which inhibit the heating of air (Boggs et al., 2022; van der Veld et al., 2019). The transition is dictated by the current and radius of the leader, among other characteristics (da Silva and Pasko, 2013). Therefore, our evidence for optically bright flashes (i.e., leader forming activity) detected by GLM up to ~ 30 km asl would require an unconventional process. One possible mechanism is that strong pressure anomalies created by the fast-rising plume (e.g., Oberhuber et al., 1998, their Figures 2–3) and its overshooting top (e.g., Luderer et al., 2007, their Figure 8) created locally higher air pressures that supported conditions for leader formation at extreme heights.

In addition to high-altitude lightning, the eruption may have produced a special class of electrical discharges known as narrow bipolar events (NBEs). NBEs are distinct from traditional lightning because they consist entirely of cold plasma (streamers). NBEs are believed to be responsible for initiating lightning, though they often occur in isolation (Rison et al., 2016). They have historically been associated with severe convection and overshooting tops in thunderclouds (Karunarathna et al., 2015; Wu et al., 2012, 2013) and produce mainly blue light (~ 337 nm) in the visible regime. Blue light is not detectable by the satellite-based GLM sensor (~ 777 nm) and could explain why there were no optical detections during the peak of the eruption—even if NBEs occurred right at the plume top, they would be invisible to GLM. Likewise, the exceptionally high peak currents detected by the ground-based networks during lightning ring activity (from 4:30–5:40, Figure S1 in Supporting Information S1) are consistent with NBEs (Le Vine, 1980; Smith et al., 1999). Some of these high-current discharges appear to follow the stratospheric cloud as it drifts downwind (white dashed outlines, Figure 2). Furthermore, our observation that traditional flash clustering algorithms do not seem to apply to these lightning data (Text S2 in Supporting Information S1) provides support for isolated electrical discharges like NBEs. Isolated, blue streamers have been photographed in a volcanic plume before (Van Eaton et al., 2022). Therefore, we remain open to the possibility that some (or all) of the “lightning rings” could be attributed to NBEs rather than lightning in the strict sense. This scenario would still imply an upper limit of ~ 30 km for traditional (optically bright) lightning in the plume, as detected by GLM. And since the highest reported altitudes of NBEs are ~ 20 km (Wu et al., 2012), the overall evidence for stratospheric electrical activity in Hunga's plume suggests that volcanic eruptions may create conditions for lightning initiation (i.e., leader and/or NBE formation) at unprecedented altitudes.

5. Conclusions

Our volcanic lightning and plume analysis reveals at least four phases of eruptive activity from 02:57 to 15:12 on 15 January 2022. In particular, the rates of proximal lightning (within 20 km of Hunga Volcano) resolve the timing and intensity of volcanic plume formation, augmenting satellite observations when the region was obscured by the upper-level cloud for several hours (especially $\sim 10:00$ – $15:00$, Figures 1 and 2). These results frame an eruptive timeline for this globally important, yet remote, eruption, with implications for monitoring volcanic hazards using real-time lightning data in the future. We expect the eruption chronology to evolve as more details from near-source observations, geological deposits, and eyewitness reports come to light.

This eruption produced the largest lightning rings ever observed (up to ~ 140 km radius). We show that the initial lightning ring matches the movement of a large-scale gravity wave in the upper umbrella cloud, formed by dramatic oscillation of the overshooting top (Figure 2, Figure S6 in Supporting Information S1). Results also indicate that the 15 January eruption produced the highest lightning rates yet documented ($> 2,600$ flashes min^{-1}). We explain the intense electrification as a function of the exceptionally high eruption rate (at least 5×10^9 kg s^{-1} including magma and external water), fast-growing umbrella cloud, and incorporation of seawater from the submarine vent. Comparison of different lightning detection technologies from spaceborne optical measurements and ground-based radio antennas constrain the height of lightning-producing regions of the volcanic plume. Based on the occurrence of optically bright flashes at high altitudes, we infer that the mixed-phase region of the volcanic plume extended up to ~ 30 km high, implying that liquid water injected deep into the stratosphere. Future

numerical simulations of the volcanic plume will be able to test the evolution and longevity of this mixed-phase microphysical region. Overall, our observations suggest that volcanic plumes can create the conditions for lightning initiation well outside the range of meteorological thunderstorms previously observed in Earth's atmosphere.

Data Availability Statement

GOES-17 and Himawari-8 data are accessible through <https://registry.opendata.aws/noaa-goes/>, <https://registry.opendata.aws/noaa-himawari/>, and NASA Worldview (<https://worldview.earthdata.nasa.gov/>). Stereoscopic cloud heights are downloadable from <https://science-data.larc.nasa.gov/LaRC-SD-Publications/2022-11-22-001-KMB/>. The data set of lightning and plume characteristics is downloadable from: <https://doi.org/10.5281/zenodo.7379584>.

Acknowledgments

Larry Mastin and two anonymous reviewers are thanked for constructive reviews. Matthew Rogers, Shane Cronin, James White, Emily Lane, Kathleen McKee, and Scott Reinhard are thanked for valuable discussions. AVE was funded by the U.S. Geological Survey Volcano Hazards Program. SAB was supported by the Laboratory Directed Research and Development program at Los Alamos National Laboratory under project number 20190107ER. KB and KK were funded by a NASA ROSES-2019 "Earth Science Research from Operational Geostationary Satellite Systems" program award. Earth Networks is thanked for providing the ENTLN and WWLLN data in this study. The scientific results and conclusions, as well as any views or opinions expressed herein, are those of the author(s) and do not necessarily reflect those of NOAA or the Department of Commerce. Any use of trade, firm, or product names is for descriptive purposes only and does not imply endorsement by the U.S. Government.

References

- Apke, J. M., Mecikalski, J. R., Bedka, K., McCaul, E. W., Homeyer, C. R., & Jewett, C. P. (2018). Relationships between deep convection updraft characteristics and satellite-based super rapid scan mesoscale atmospheric motion vector-derived flow. *Monthly Weather Review*, 146(10), 3461–3480. <https://doi.org/10.1175/mwr-d-18-0119.1>
- Astafyeva, E., Maletskii, B., Mikesell, T. D., Munaibari, E., Ravanelli, M., Coisson, P., et al. (2022). The 15 January 2022 Hunga Tonga eruption history as inferred from ionospheric observations. *Geophysical Research Letters*, 49(10), e2022GL098827. <https://doi.org/10.1029/2022GL098827>
- Behnke, S. A., & Bruning, E. C. (2015). Changes to the turbulent kinematics of a volcanic plume inferred from lightning data. *Geophysical Research Letters*, 42(10), 4232–4239. <https://doi.org/10.1002/2015gl064199>
- Behnke, S. A., Thomas, R. J., McNutt, S. R., Schneider, D. J., Krehbiel, P. R., Rison, W., & Edens, H. E. (2013). Observations of volcanic lightning during the 2009 eruption of Redoubt Volcano. *Journal of Volcanology and Geothermal Research*, 259, 214–234. <https://doi.org/10.1016/j.jvolgeores.2011.12.010>
- Boggs, L. D., Mach, D., Bruning, E., Liu, N., Van der Velde, O. A., Montanyá, J., et al. (2022). Upward propagation of gigantic jets revealed by 3D radio and optical mapping. *Science Advances*, 8(31), eabl8731. <https://doi.org/10.1126/sciadv.abl8731>
- Bonadonna, C., & Phillips, J. C. (2003). Sedimentation from strong volcanic plumes. *Journal of Geophysical Research*, 108(B7), 2340. <https://doi.org/10.1029/2002JB002034>
- Briggs, M. S., Lesage, S., Schultz, C., Mailyan, B., & Holzworth, R. H. (2022). A terrestrial gamma-ray flash from the 2022 Hunga Tonga–Hunga Ha'apai volcanic eruption. *Geophysical Research Letters*, 49(14). <https://doi.org/10.1029/2022gl099660>
- Bruning, E. C., & MacGorman, D. R. (2013). Theory and observations of controls on lightning flash size spectra. *Journal of the Atmospheric Sciences*, 70(12), 4012–4029. <https://doi.org/10.1175/jas-d-12-0289.1>
- Calhoun, K. M., MacGorman, D. R., Ziegler, C. L., & Biggerstaff, M. I. (2013). Evolution of lightning activity and storm charge relative to dual-Doppler analysis of a high-precipitation supercell storm. *Monthly Weather Review*, 141(7), 2199–2223. <https://doi.org/10.1175/MWR-D-12-00258.1>
- Calhoun, K. M., Mansell, E. R., MacGorman, D. R., & Dowell, D. C. (2014). Numerical simulations of lightning and storm charge of the 29–30 May 2004 Geary, Oklahoma, supercell thunderstorm using EnKF mobile radar data assimilation. *Monthly Weather Review*, 142(11), 3977–3997. <https://doi.org/10.1175/mwr-d-13-00403.1>
- Carr, S. A., Krotkov, N. A., Fisher, B. L., & Li, C. (2022). Out of the blue: Volcanic SO₂ emissions during the 2021–2022 eruptions of Hunga Tonga–Hunga Ha'apai (Tonga). *Frontiers of Earth Science*, 10. <https://doi.org/10.3389/feart.2022.976962>
- Carr, J. L., Horváth, Á., Wu, D. L., & Friberg, M. D. (2022). Stereo plume height and motion retrievals for the record-setting Hunga Tonga–Hunga Ha'apai eruption of 15 January 2022. *Geophysical Research Letters*, 49(9). <https://doi.org/10.1029/2022gl098131>
- Cimarelli, C., Behnke, S. A., Genareau, K., Méndez Harper, J. S., & Van Eaton, A. R. (2022). Volcanic electrification: Recent advances and future perspectives. *Bulletin of Volcanology*, 84(78), 78. <https://doi.org/10.1007/s00445-022-01591-3>
- Cummins, K. L. (2021). On the spatial and temporal variation of GLM flash detection and how to manage it. In *Paper presented at the American meteorological society 101st annual meeting, virtual*. Retrieved from <https://ams.confex.com/ams/101ANNUAL/meetingapp.cgi/Paper/382589>
- Cummins, K. L., Murphy, M. J., Bardo, E. A., Hiscox, W. L., Pyle, R. B., & Pifer, A. E. (1998). A combined TOA/MDF technology upgrade of the U.S. National lightning detection network. *Journal of Geophysical Research*, 103(D8), 9035–9044. <https://doi.org/10.1029/98JD00153>
- Da Silva, C. L., & Pasko, V. P. (2013). Dynamics of streamer-to-leader transition at reduced air densities and its implications for propagation of lightning leaders and gigantic jets. *Journal of Geophysical Research: Atmospheres*, 118(24), 13561–13590. <https://doi.org/10.1002/2013JD020618>
- Deierling, W., Petersen, W. A., Latham, J., Ellis, S., & Christian, H. J. (2008). The relationship between lightning activity and ice fluxes in thunderstorms. *Journal of Geophysical Research*, 113(D15), D15210. <https://doi.org/10.1029/2007jd009700>
- DiGangi, E. A., MacGorman, D. R., Ziegler, C. L., Betten, D., Biggerstaff, M., Bowlan, M., & Potvin, C. K. (2016). An overview of the 29 May 2012 Kingfisher supercell during DC3. *Journal of Geophysical Research: Atmospheres*, 121(24), 14316–14343. <https://doi.org/10.1002/2016JD025690>
- Dwyer, J. R., & Uman, M. A. (2014). The physics of lightning. *Physics Reports*, 534(4), 147–241. <https://doi.org/10.1016/j.physrep.2013.09.004>
- Gavrilov, B. G., Poklad, Y. V., Ryakhovsky, I. A., Ermak, V. M., Achkasov, N. S., & Kozakova, E. N. (2022). Global electromagnetic disturbances caused by the eruption of the Tonga volcano on January 15, 2022. *Journal of Geophysical Research: Atmospheres*, 127(23), e2022JD037411. <https://doi.org/10.1029/2022JD037411>
- Gupta, A. K., Bennartz, R., Fauria, K. E., & Mittal, T. (2022). Eruption chronology of the December 2021 to January 2022 Hunga Tonga–Hunga Ha'apai eruption sequence. *Communications Earth & Environment*, 3(314), 314. <https://doi.org/10.1038/s43247-022-00606-3>
- Herzog, M., & Graf, H.-F. (2010). Applying the three-dimensional model ATHAM to volcanic plumes: Dynamics of large co-ignimbrite eruptions and associated injection heights for volcanic gases. *Geophysical Research Letters*, 37(19), L19807. <https://doi.org/10.1029/2010GL044986>
- Holasek, R. E., Self, S., & Woods, A. W. (1996). Satellite observations and interpretation of the 1991 Mount Pinatubo eruption plumes. *Journal of Geophysical Research*, 101(B12), 27635–27655. <https://doi.org/10.1029/96JB01179>

- Karunaratna, N., Marshall, T. C., Stolzenburg, M., & Karunaratne, S. (2015). Narrow bipolar pulse locations compared to thunderstorm radar echo structure. *Journal of Geophysical Research: Atmospheres*, 120(22), 11690–11706. <https://doi.org/10.1002/2015JD023829>
- Koyaguchi, T., & Woods, A. W. (1996). On the formation of eruption columns following explosive mixing of magma and surface-water. *Journal of Geophysical Research*, 101(B3), 5561–5574. <https://doi.org/10.1029/95JB01687>
- Krehbiel, P. R., Rioussel, J. A., Pasko, V. P., Thomas, R. J., Rison, W., Stanley, M. A., & Edens, H. E. (2008). Upward electrical discharges from thunderstorms. *Nature Geoscience*, 1(4), 233–237. <https://doi.org/10.1038/ngeo162>
- Kulman, K. M., Ziegler, C. L., Mansell, E. R., MacGorman, D. R., & Straka, J. M. (2006). Numerically simulated electrification and lightning of the 29 June 2000 STEPS supercell storm. *Monthly Weather Review*, 134(10), 2734–2757. <https://doi.org/10.1175/MWR3217.1>
- Le Vine, D. M. (1980). Sources of the strongest RF radiation from lightning. *Journal of Geophysical Research*, 85(C7), 4091–4095. <https://doi.org/10.1029/jc085ic07p04091>
- Ludering, G., Trentmann, J., Hungershofer, K., Herzog, M., Fromm, M., & Andreae, M. O. (2007). Small-scale mixing processes enhancing troposphere-to-stratosphere transport by pyro-cumulonimbus storms. *Atmospheric Chemistry and Physics*, 7(23), 5945–5957. <https://doi.org/10.5194/acp-7-5945-2007>
- MacGorman, D. R., Elliott, M. S., & DiGangi, E. (2017). Electrical discharges in the overshooting tops of thunderstorms. *Journal of Geophysical Research: Atmospheres*, 122(5), 2929–2957. <https://doi.org/10.1002/2016JD025933>
- Mather, T. A., & Harrison, R. G. (2006). Electrification of volcanic plumes. *Surveys in Geophysics*, 27(4), 387–432. <https://doi.org/10.1007/s10712-006-9007-2>
- Matoza, R. S., Fee, D., Assink, J. D., Iezzi, A. M., Green, D. N., Kim, K., et al. (2022). Atmospheric waves and global seismoacoustic observations of the January 2022 Hunga eruption, Tonga. *Science*, 377(6601), 95–100. <https://doi.org/10.1126/science.abo7063>
- Millán, L., Santee, M. L., Lambert, A., Livesey, N. J., Werner, F., Schwartz, M. J., et al. (2022). The Hunga Tonga-Hunga Ha'apai hydration of the stratosphere. *Geophysical Research Letters*, 49(13), e2022GL099381. <https://doi.org/10.1029/2022GL099381>
- Oberhuber, J. M., Herzog, M., Graf, H. F., & Schwanke, K. (1998). Volcanic plume simulation on large scales. *Journal of Volcanology and Geothermal Research*, 87(1–4), 29–53. [https://doi.org/10.1016/s0377-0273\(98\)00099-7](https://doi.org/10.1016/s0377-0273(98)00099-7)
- Omira, R., Ramalho, R. S., Kim, J., Gonzalez, P. J., Kadri, U., Miranda, J. M., et al. (2022). Global Tonga tsunami explained by a fast-moving atmospheric source. *Nature*, 609(7928), 734–740. <https://doi.org/10.1038/s41586-022-04926-4>
- Oppenheimer, C. (1998). Volcanological applications of meteorological satellites. *International Journal of Remote Sensing*, 19(15), 2829–2864. <https://doi.org/10.1080/014311698214307>
- Pavlonis, M. J., Sieglaff, J., & Cintineo, J. (2018). Automated detection explosive volcanic eruptions using satellite-derived cloud vertical growth rates. *Earth and Space Science*, 5(12), 903–928. <https://doi.org/10.1029/2018EA000410>
- Payne, C. D., Schuur, T. J., MacGorman, D. R., Biggerstaff, M. I., Kuhlman, K. M., & Rust, W. D. (2010). Polarimetric and electrical characteristics of a lightning ring in a supercell storm. *Monthly Weather Review*, 138(6), 2405–2425. <https://doi.org/10.1175/2009mwr3210.1>
- Podglajen, A., Le Pichon, A., Garcia, R. F., G  rier, S., Millet, C., Bedka, K., et al. (2022). Stratospheric balloon observations of infrasound waves from the 15 January 2022 Hunga Eruption, Tonga. *Geophysical Research Letters*, 49(19), e2022GL100833. <https://doi.org/10.1029/2022gl100833>
- Prata, A. T., Folch, A., Prata, A. J., Biondi, R., Brenot, H., Cimorelli, C., et al. (2020). Anak Krakatau triggers volcanic freezer in the upper troposphere. *Scientific Reports*, 10(1), 3584. <https://doi.org/10.1038/s41598-020-60465-w>
- Proud, S. R., Prata, A. T., & Schma  , S. (2022). The January 2022 eruption of Hunga Tonga-Hunga Ha'apai volcano reached the mesosphere. *Science*, 378(6619), 554–556. <https://doi.org/10.1126/science.abo4076>
- Purkis, S. J., Ward, S. N., Fitzpatrick, N. M., Garven, J. B., Slayback, D., Cronin, S. J., et al. (2023). The 2022 Hunga-Tonga megatsunami: Near-field simulation of a once-in-a-century event. *Science Advances*, 9(15), ead5493. <https://doi.org/10.1126/sciadv.adf5493>
- Quick, M. G., & Krider, E. P. (2013). Optical power and energy radiated by natural lightning. *Journal of Geophysical Research: Atmospheres*, 118(4), 1868–1879. <https://doi.org/10.1002/jgrd.50182>
- Rison, W., Krehbiel, P. R., Stock, M. G., Edens, H. E., Shao, X.-M., Thomas, R. J., et al. (2016). Observations of narrow bipolar events reveal how lightning is initiated in thunderstorms. *Nature Communications*, 7(1), 10721. <https://doi.org/10.1038/ncomms10721>
- Schultz, C. J., Andrews, V. P., Genareau, K. D., & Naeger, A. R. (2020). Observations of lightning in relation to transitions in volcanic activity during the 3 June 2018 Fuego Eruption. *Scientific Reports*, 10(1), 18015. <https://doi.org/10.1038/s41598-020-74576-x>
- Sellitto, P., Podglajen, A., Belhadji, R., Boichu, M., Carboni, E., Cuesta, J., et al. (2022). The unexpected radiative impact of the Hunga Tonga eruption of 15th January 2022. *Communications Earth & Environment*, 3(1), 288. <https://doi.org/10.1038/s43247-022-00618-z>
- Smith, C. M., Gaudin, D., Van Eaton, A. R., Behnke, S. A., Reader, S., Thomas, R. J., et al. (2021). Impulsive volcanic plumes generate volcanic lightning and vent discharges: A statistical analysis of Sakurajima Volcano in 2015. *Geophysical Research Letters*, 48(11), e2020GL092323. <https://doi.org/10.1029/2020gl092323>
- Smith, D. A., Shao, X. M., Holden, D. N., Rhodes, C. T., Brook, M., Krehbiel, P. R., et al. (1999). A distinct class of isolated intracloud lightning discharges and their associated radio emissions. *Journal of Geophysical Research*, 104(D4), 4189–4212. <https://doi.org/10.1029/1998jd200045>
- Sparks, R. S. J., Bursik, M. I., Carey, S. N., Gilbert, J. E., Glaze, L., Sigurdsson, H., & Woods, A. W. (1997). *Volcanic plumes*. John Wiley.
- Textor, C., Graf, H.-F., Herzog, M., Oberhuber, J. M., Rose, W. I., & Ernst, G. G. J. (2006). Volcanic particle aggregation in explosive eruption columns. Part II: Numerical experiments. *Journal of Volcanology and Geothermal Research*, 150(4), 378–394. <https://doi.org/10.1016/j.jvolgeores.2005.09.008>
- van der Velde, O. A., Montany  , J., L  pez, J. A., & Cummer, S. A. (2019). Gigantic jet discharges evolve stepwise through the middle atmosphere. *Nature Communications*, 10(1), 1–10. <https://doi.org/10.1038/s41467-019-12261-y>
- Van Eaton, A., Behnke, S., Lapierre, J., Vagasky, C., Schultz, C., Pavlonis, M., et al. (2023). Lightning and volcanic plume data from the climactic eruption of Hunga Volcano, Tonga, in January 2022 (Version 1) [Dataset]. Zenodo. <https://doi.org/10.5281/zenodo.7379584>
- Van Eaton, A. R., Herzog, M., Wilson, C. J. N., & McGregor, J. (2012). Ascent dynamics of large phreatomagmatic eruption clouds: The role of microphysics. *Journal of Geophysical Research*, 117(B3), B03203. <https://doi.org/10.1029/2011JB008892>
- Van Eaton, A. R., Schneider, D. J., Smith, C. M., Haney, M. M., Lyons, J. J., Said, R., et al. (2020). Did ice-charging generate volcanic lightning during the 2016–2017 eruption of Bogoslof volcano, Alaska? *Bulletin of Volcanology*, 80(24), 24. <https://doi.org/10.1007/s00445-019-1350-5>
- Van Eaton, A. R., Smith, C. M., Pavlonis, M., & Said, R. (2022). Eruption dynamics leading to a volcanic thunderstorm—The January 2020 eruption of Taal volcano, Philippines. *Geology*, 50(4), 491–495. <https://doi.org/10.1130/G49490.1>
- Vergoz, J., Hupe, P., Listowski, C., Le Pichon, A., Garc  s, M. A., Marchetti, E., et al. (2022). IMS observations of infrasound and acoustic-gravity waves produced by the January 2022 volcanic eruption of Hunga, Tonga: A global analysis. *Earth and Planetary Science Letters*, 591, 117639. <https://doi.org/10.1016/j.epsl.2022.117639>
- V  mel, H., Evan, S., & Tully, M. (2022). Water vapor injection into the stratosphere by Hunga Tonga-Hunga Ha'apai. *Science*, 377(6613), 1444–1447. <https://doi.org/10.1126/science.abq2299>

- Woods, A. W. (1995). The dynamics of explosive volcanic eruptions. *Reviews of Geophysics*, 33(4), 495–530. <https://doi.org/10.1029/95rg02096>
- Wu, T., Dong, W., Zhang, Y., Funaki, T., Yoshida, S., Morimoto, T., et al. (2012). Discharge height of lightning narrow bipolar events. *Journal of Geophysical Research*, 117(D5), D05119. <https://doi.org/10.1029/2011JD017054>
- Wu, T., Takayanagi, Y., Yoshida, S., Funaki, T., Ushio, T., & Kawasaki, Z. (2013). Spatial relationship between lightning narrow bipolar events and parent thunderstorms as revealed by phased array radar. *Geophysical Research Letters*, 40(3), 618–623. <https://doi.org/10.1002/grl.50112>

References From the Supporting Information

- Bateman, M., & Mach, D. (2022). Preliminary detection efficiency and false alarm rate assessment of the Geostationary Lightning Mapper on the GOES-16 satellite. *Journal of Applied Remote Sensing*, 14(3), 032406. <https://doi.org/10.1117/1.JRS.14.032406>
- Bruning, E. C., Tillier, C. E., Edgington, S. F., Rudlosky, S. D., Zajic, J., Gravelle, C., et al. (2019). Meteorological imagery for the geostationary lightning mapper. *Journal of Geophysical Research: Atmospheres*, 124(24), 14285–14309. <https://doi.org/10.1029/2019JD030874>
- Brunner, K. N., & Bitzer, P. M. (2020). A first look at cloud inhomogeneity and its effect on lightning optical emission. *Geophysical Research Letters*, 47(10), e2020GL087094. <https://doi.org/10.1029/2020GL087094>
- Costa, A., Folch, A., & Macedonio, G. (2013). Density-driven transport in the umbrella region of volcanic clouds: Implications for tephra dispersion models [Erratum published 17 Jun 2019]. *Geophysical Research Letters*, 40(18), 4823–4827. <https://doi.org/10.1002/grl.50942>
- Goodman, S. J., Cecil, D. J., & Arnold, J. E. (2002). The most extreme thunderstorms on Earth. In *Paper presented at the 17th international lightning detection conference*.
- Mastin, L. G., & Van Eaton, A. R. (2020). Comparing simulations of umbrella-cloud growth and ash transport with observations from Pinatubo, Kelud, and Calbuco Volcanoes. *Atmosphere*, 11(10), 1038. <https://doi.org/10.3390/atmos11101038>
- Nag, A., Murphy, M. J., Schulz, W., & Cummins, K. L. (2015). Lightning locating systems: Insights on characteristics and validation techniques. *Earth and Space Science*, 2(4), 65–93. <https://doi.org/10.1002/2014EA000051>
- Pouget, S., Bursik, M., Webley, P., Dehn, J., & Pavolonis, M. (2013). Estimation of eruption source parameters from umbrella cloud or downwind plume growth rate. *Journal of Volcanology and Geothermal Research*, 258, 100–112. <https://doi.org/10.1016/j.jvolgeores.2013.04.002>
- Rodger, C. J., Werner, S., Brundell, J. B., Lay, E. H., Thomson, N. R., Holzworth, R. H., & Dowden, R. L. (2006). Detection efficiency of the VLF world-wide lightning location network (WWLLN): Initial case study. *Annales Geophysicae*, 24(12), 3197–3214. <https://doi.org/10.5194/angeo-24-3197-2006>
- Said, R. K. (2017). Towards a global lightning locating system. *Weather*, 72(2), 36–40. <https://doi.org/10.1002/wea.2952>
- Said, R. K. (2021). Improved GLD360 location accuracy and peak current estimates with empirically determined VLF propagation parameters. In *Paper presented at the 10th conference on the meteorological application of lightning data*. American Meteorological Society.
- Said, R. K., Inan, U. S., & Cummins, K. L. (2010). Long-range lightning geolocation using a VLF radio atmospheric waveform bank. *Journal of Geophysical Research*, 115(D23), D23108. <https://doi.org/10.1029/2010JD013863>
- Suzuki, Y. J., & Koyaguchi, T. (2009). A three-dimensional numerical simulation of spreading umbrella clouds. *Journal of Geophysical Research*, 114(B3), B03209. <https://doi.org/10.1029/2007jb005369>
- Vagasky, C. (2017). Enveloped eyewall lightning: The EEL signature in tropical cyclones. *Journal of Operational Meteorology*, 5(14), 171–179. <https://doi.org/10.15191/nwajom.2017.0514>
- Vagasky, C., & Said, R. K. (2022). Did the eruption of Hunga Tonga-Hunga Ha'apai produce the greatest concentration of lightning ever detected? In *Paper presented at the 2022 American geophysical union fall meeting*.
- Vagasky, C., Said, R., & Krippner, J. (2021). Observations of volcanic lightning using GLD360. In *Paper presented at the American meteorological society 101st annual meeting, virtual*. Retrieved from <https://ams.confex.com/ams/101ANNUAL/meetingapp.cgi/Paper/382669>
- Webster, H. N., Devenish, B. J., Mastin, L. G., Thomson, D. J., & Van Eaton, A. R. (2020). Operational modelling of umbrella cloud growth in a Lagrangian volcanic ash transport and dispersion model. *Atmosphere*, 11(2), 200. <https://doi.org/10.3390/atmos11020200>
- Williams, E., Boldi, B., Matlin, A., Weber, M., Hodanish, S., Sharp, D., et al. (1999). The behavior of total lightning activity in severe Florida thunderstorms. *Atmospheric Research*, 51(3), 245–265. [https://doi.org/10.1016/S0169-8095\(99\)00011-3](https://doi.org/10.1016/S0169-8095(99)00011-3)
- Zhu, Y., Stock, M., Lapierre, J., & DiGangi, E. (2022). Upgrades of the Earth networks total lightning network in 2021. *Remote Sensing*, 14(9), 2209. <https://doi.org/10.3390/rs14092209>